Supramolecular chemistry on water – towards self-assembling molecular electronic circuitry

Kasper Nørgaard and Thomas Bjørnholm*

Received (in Cambridge, UK) 17th November 2004, Accepted 8th February 2005
First published as an Advance Article on the web 1st March 2005
DOI: 10.1039/b417526n

This *feature article* describes the self-assembly of electroactive molecules at the air/water interface, emphasizing the structural and electronic characterizations of the resulting supramolecular architectures.

Introduction

The term *supramolecular chemistry* was introduced by 1987 Nobel laureate J.-M. Lehn in 1978,[1] thereby launching a new field of interdisciplinary scientific research. Supramolecular chemistry can be described as chemistry beyond the covalent bond, as it relates to the collective properties of assemblies of individual molecules through intermolecular interactions. These properties are determined by the spatial configuration of the constituent molecules and the nature of the intermolecular bonds between them in addition to the intrinsic properties of each individual molecule.

For more than a century, synthetic organic chemists have accumulated an immense amount of knowledge about the rules that govern the fabrication and transformation of covalent molecular species. The level of understanding has presently reached a stage where even very complex organic target molecules can be synthesized. In contrast to this mature branch of chemistry the field of supramolecular self-assembly is still in its infancy, since the ability to design and arrange individual molecular building blocks into pre-programmed and well-defined architectures is very limited. These limitations are imposed by the spatial complexity and relative weakness of the intermolecular interactions that determine the supramolecular structure, that is electrostatic forces, hydrogen bonding, π–π stacking, van der Waals interactions and the hydrophobic effect. The strength of these interactions is usually only a small fraction of that of a covalent bond ($\approx$350 kJ mol^{-1}) and supramolecular species are therefore generally more labile, adaptive and flexible but less stable than their molecular constituents.

Self-assembled systems have an intrinsic propensity towards the spontaneous formation of extensive ordered molecular arrays, consisting of relatively simple molecular building blocks held together by an appropriate balance between intermolecular non-covalent forces and the surrounding media. The self-assembly process thus relies on mutual recognition between complementary supramolecular building blocks through non-covalent interactions.

Self-assembled systems are ubiquitous in Nature, the eukaryotic cell-membrane, double-stranded DNA helix and the α-helix and β-pleated sheat of polypeptides being prominent examples. Yet, the self-assembly of artificial functional molecular systems still remains a major challenge to the supramolecular chemist. Nonetheless, supramolecular self-assembly has often been proclaimed to hold the key to nanoscale engineering. Where technological and physical limitations may soon prevent the continuing miniaturization of *e.g.* electronic devices *via* current ''top-down'' lithographic approaches, supramolecular self-assembly addresses the fundamental challenge of fabricating ordered nanoscale structures *via* a ''bottom-up'' approach.

Whereas self-assembly in solution can be regarded as a thermodynamically controlled reversible equilibrium process, self-assembly of crystals is essentially a nonequilibrium situation where both kinetic and thermodynamical aspects contribute to the resulting supramolecular structure. This means that crystal structure predictions of even simple molecules are virtually impossible,[2] which considerably complicates the field of *crystal engineering*[3] – *i.e.* the rational design and preparation of crystalline materials, based on a consideration of steric and topological aspects of the constituent building blocks as well as their intermolecular bonding properties. Still, a major driving force in the field of crystal engineering is the aspiration to fabricate solid state molecular devices (electronic, optical or magnetic) based on self-assembly principles.

In recent years, an intense research effort has focused on the fabrication of molecular electronic devices, such as light

*tb@nano.ku.dk

Dr Kasper Nørgaard was born in 1974 and graduated in Chemistry from the University of Copenhagen in 2000, where he also recently concluded his PhD work on ''Supramolecular Surface Chemistry'' under the supervision of Prof. Thomas Bjørnholm. His present research activities include supramolecular chemistry, X-ray physics, nanoparticle synthesis, Langmuir–Blodgett films and molecular electronics.

Dr Thomas Bjørnholm is Professor of Materials Chemistry and director of the Nano-Science Center at the University of Copenhagen. He was born in 1960 and received his PhD degree from the University of Copenhagen in 1990. He was a post doctoral associate at the UCSD with Profs. M. B. Maple and I. K. Schuller, and was a visiting professor at the University of Texas at Austin in 1997. Current research interests include molecular electronics, supramolecular chemistry, bio-nanotechnology, Langmuir–Blodgett films and nanochemistry.

 This journal is © The Royal Society of Chemistry 2005

emitting diodes (LEDs),[4] field effect transistors (FETs)[5] and photovoltaic cells,[6] based on π-conjugated organic molecules.[7]

Much of the current interest in organic-based molecular electronics was sparked by the 1977 discovery of electronic conductivity in halogen-doped polyacetylene by Shirakawa *et al.*[8] and, a few years later, the conducting and superconducting charge-transfer "*Bechgaard salts*",[9] consisting of stacks of cationic tetramethyltetraselenafulvalenes (*e.g.* $(TMTSF)_2PF_6$). Electronic conductivity in these materials is facilitated by the extended delocalized π-electron systems arising from the overlap of π-orbitals, either intramolecularly (*e.g.* along the polymer-backbone in polyacetylene) or intermolecularly (*e.g.* along the stacking direction of the TMTSF units in $(TMTSF)_2PF_6$).

The macroscopic conductivity, σ, of a material can be described in terms of the mobility, μ, and density, n, of the charge carriers (electrons or holes) by the expression:

$$\sigma = n\mu q \quad (1)$$

where q is the nominal charge of the charge carriers. For a material to display appreciable conductivity, it must thus possess a substantial number of charge carriers in addition to a suitable route to their migration in the material. However, most organic materials have very low charge carrier concentrations, unless additional charge carriers are introduced into the material by doping. In addition, the charge carrier mobility of a material is closely related to its structure, and highly ordered structures are a prerequisite for achieving high carrier mobilities. The presence of packing defects and boundaries between well-ordered domains contributes to a reduction of the overall carrier mobility, which emphasizes the need to control the structure not only on the molecular scale, but also on the nano- and micrometer scales.

In order to face some of the challenges associated with the crystal engineering of novel supramolecular architectures with interesting electronic properties and to gain insight into the general processes that govern the self-assembly of molecular synthons, the need to divide this intricate problem into simpler sub-tasks becomes evident. One approach is to reduce the effective dimensionality of the system, for example by confining the system to an interface, combined with the study of gradually more complex molecular building blocks. In this respect, the interface between air and water offers some advantages as a model system for studies of two-dimensional supramolecular self-assembly processes, as it forms a well-defined, ideally flat and homogeneous experimental situation.[10] Developments in surface specific characterization techniques have further advanced the structural analysis of supramolecular assemblies at interfaces (*vide infra*).

The present article focuses on the rational design and self-assembly of supramolecular electroactive structures at the air/water interface. The first step involves an understanding of the factors that contribute to the packing of molecules at the interface. This is done by studying a series of molecules, starting from (i) a simple long-chain *n*-alkane, (ii) adding a hydrophilic head-group to the alkane, (iii) replacing the head-group with an electroactive moiety, (iv) linking the electroactive headgroups into a π-conjugated polymer, (v) changing the π-conjugation to a large discotic system, and finally (vi) a π-conjugated system without alkyl-substituents. This approach is illustrated schematically in Fig. 1.

The second step involves the study of the intrinsic electronic properties of the self-assembled structures and the properties of novel self-assembled architectures arising through a supramolecular synthesis of the different molecular building blocks at the air/water interface.

Self-assembly at the air/water interface

Langmuir films are monomolecular layers of surface-active molecules (*surfactants*) floating at the interface between a gas and a liquid phase. Such monolayers are thermodynamically stable due to intermolecular forces between the molecules in the layer as well as through a balance between lyophilic and lyophobic forces, which tend to respectively maximize and minimize the contact area between the liquid and specific parts of the molecules. Molecules which consist of both solvent-attracting and solvent-repelling moieties are generally termed *amphiphilic*.

Langmuir films are named after the 1932 Nobel laureate Irwin Langmuir,[11] who was among the first to perform systematic studies of the physical-chemical properties of insoluble monolayers of organic surfactants on water surfaces. Based on experimental work on adsorbate-induced reduction of the surface tension of liquids, he introduced the term *surface pressure*, Π, a two-dimensional equivalent to pressure, defined as the difference between the surface tension of pure solvent, γ_0, and the experimentally measured surface tension of solvent including surfactant, γ (*i.e.* $\Pi \equiv \gamma_0 - \gamma$).

When simple amphiphilic surfactants—such as long-chain fatty acids—are spread on the water surface of a simple trough, they form monolayers in which the hydrophilic carboxylic acid moieties are submersed in the water phase, resulting in an overall orientation of the molecules parallel to the surface normal. Using one or more movable barriers in the trough, the accessible surface area of the surfactants can be

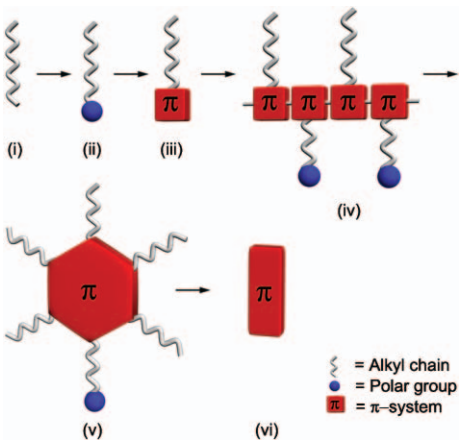

Fig. 1 Schematic illustration of the different molecular building blocks included in this study: (i) a long-chain *n*-alkane, (ii) a simple amphiphile, (iii) an amphiphilic molecule with an electroactive head-group, (iv) an amphiphilic π-conjugated polymer, (v) a discotic π-conjugated amphiphile and (vi) a π-conjugated oligomer.

controlled, which in combination with surface pressure measurements allows the pressure–area relationship of a given surfactant to be determined. Langmuir's co-worker, Katherine Blodgett, later discovered that consecutive monolayers of surfactants could be transferred onto a solid substrate by repeatedly dipping the substrate vertically through the water surface while maintaining a constant surface pressure.[12] This method for multilayer fabrication has since been known as the Langmuir–Blodgett (LB) technique, which is illustrated schematically in Fig. 2. The produced multilayer films can have different molecular orientations of each layer, depending on the exact details of the dipping process.[13]

The opportunity for direct imaging and structural studies of molecules at the nanoscale has increased tremendously in the last two decades. With the development of high intensity X-rays from synchrotron undulator beamlines the possibility to perform diffraction experiments directly on monomolecular films emerged.[14–16] This allows the lateral crystalline structure of the films to be elucidated. In combination with scanning probe techniques, such as atomic force microscopy,[17] applied to substrate-transferred films these methods provide a very powerful set of tools, which allow the molecular structure of the individual amphiphiles to be related to the resulting supramolecular structure of the films assembled at the air/water interface.

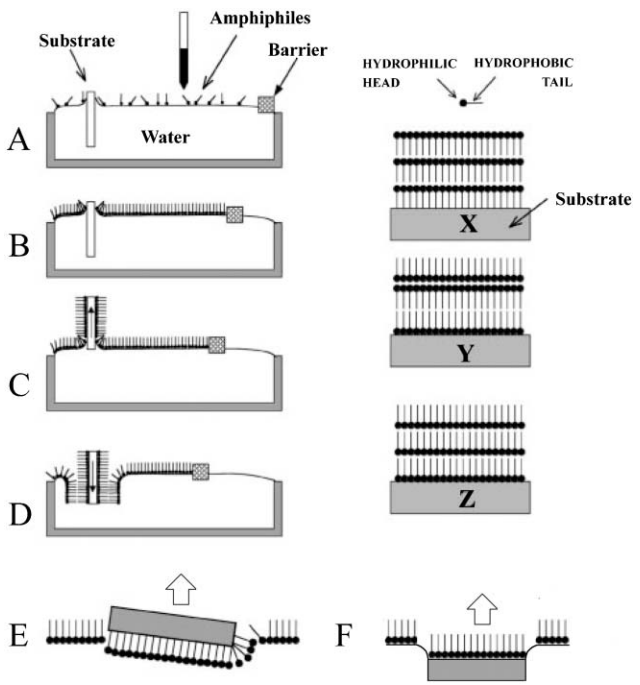

Fig. 2 The Langmuir–Blodgett technique. Left: A, deposition of the amphiphiles on the water surface with a solid substrate submerged; B, compression of the monolayer by the barrier(s); C, vertical transfer of the monolayer by pulling out the substrate; D, multilayer build-up by repeated up and down strokes of the substrate; E, monolayer transfer by horizontal dipping; F, horizontal lifting. Right: examples of different types of multilayer structures (X, Y and Z) which can be built by the LB technique.

Structural characterization methods

The wavelength of X-rays ($\lambda \approx 1$ Å) is the same order of magnitude as chemical bonds, which suggests that they can be used to obtain direct information about molecular organisation even in monomolecular layers at interfaces.

Surface sensitive X-ray scattering can be measured in two distinct geometries: grazing-incidence X-ray diffraction (GIXD) and specular X-ray reflectivity (XR). The experimental setup is shown schematically in Fig. 3. GIXD probes the lateral lattice symmetry and structure parameters of crystalline domains in a monolayer or thin film. The experiments utilize the fact that below a certain *critical angle*, α_c, total external reflection of the X-rays takes place. This is a result of the refractive index of materials being less than unity in the X-ray wavelength region. For the air/water interface the critical angle is $\alpha_c = 0.13^\circ$ for a wavelength $\lambda = 1.3$ Å. An incidence angle slightly below this value, *e.g.* $\alpha_i = 0.85\ \alpha_c$, will cause the X-rays to penetrate less than 100 Å beneath the interface, resulting in a greatly enhanced surface sensitivity. The diffracted intensity is recorded as a function of the horizontal scattering angle, $2\theta_{xy}$, along with its vertical component, α_f. Since the crystalline domains are oriented randomly around the surface normal, GIXD can be considered a surface analogue to 3D powder diffraction.

X-ray reflectivity is used to obtain information about the vertical structure of thin films. The incident angle is varied while the reflected intensity is measured at $\alpha_f = \alpha_i$ and $2\theta_{xy} = 0$. The normalized reflectivity data $R(q_z)/R_F(q_z)$, where $R_F(q_z)$ is the Fresnel reflectivity from a perfectly sharp interface, can be inverted to yield the laterally averaged electron density across the interface, $\rho(z)$. This data inversion can be done by a model-independent method[18] or alternatively by use of a (often simplified) molecular model of the interfacial region.[14,15] Unlike diffraction experiments, XR does not require any crystallinity in the film, and it gives a quantitative measure of all electrons in a sample.

Paraffin and the hydrophobic effect

The hydrophobic effect plays an important role for a wide range of phenomena such as protein folding, lipid aggregation, forces between hydrophobic surfaces in water and chemical self-assembly.[19] For highly curved surfaces, the hydrophobic effect is believed to be largely entropic in nature, since it relies on the forced ordering of water molecules (through hydrogen bonds) around non-polar surfaces. Minimization of the unfavourable loss in entropy obtained from this ordering

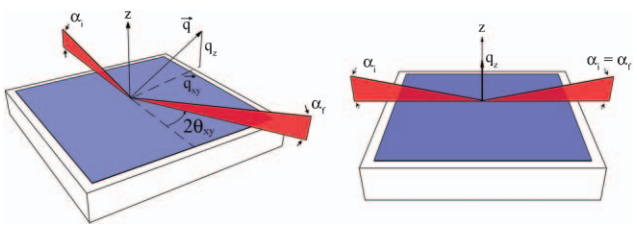

Fig. 3 Schematic illustrations of the two surface sensitive X-ray scattering geometries. Left: Grazing-incidence X-ray diffraction. Right: Specular X-ray reflectivity.

This journal is © The Royal Society of Chemistry 2005

results in a minimization also of the contact area between the aqueous and the non-polar media.[20]

For extended hydrophobic surfaces in contact with water hydrogen bonding is depleted, which leads to a drying of the interface – a phenomenon known as dewetting. While dewetting has previously been treated theoretically,[21] the first experimental evidence of dewetting of a hydrophobic surface in contact with water was based on X-ray reflectivity measurements on a Langmuir monolayer of paraffin.[22]

Despite not being amphiphiles, long-chain perfluorinated and non-fluorinated *n*-alkanes have been shown to form Langmuir monolayers on a water surface. Rice *et al*[23] reported the formation of ordered Langmuir monolayers of perfluoro-*n*-eicosane ($C_{20}F_{42}$). GIXD investigations revealed a vertical alignment of the molecules in a 2D crystalline, hexagonal packing arrangement at the air/water interface. Non-fluorinated paraffin (n-$C_{36}H_{74}$) has similarly been shown to form crystalline monolayers on water.[24] It is suggested that van der Waals forces alone are sufficient to stabilise monolayers of these highly hydrophobic molecules. The paraffin monolayer is a static polycrystalline film.

Fig. 4 shows the measured X-ray reflectivity for a Langmuir monolayer of paraffin, as well as the normalized electron density profile $\rho(z)/\rho_{water}$ across the interface corresponding to these data. The shaded area in Fig. 4B indicates a decrease in the density down to about $\rho(z)/\rho_{water} = 0.9$ occurring at the alkane/water interface. This contact region with low water density has a half width of 8–10 Å and this density deficit is due to a significant dewetting of the contact region between the water and alkane.

This dewetting phenomenon does not occur in monolayers of molecules that are terminated at one end by a single polar group such as a carboxylic acid or a hydroxy group, and hence depend critically on the hydrophobicity of the solid surface.[22]

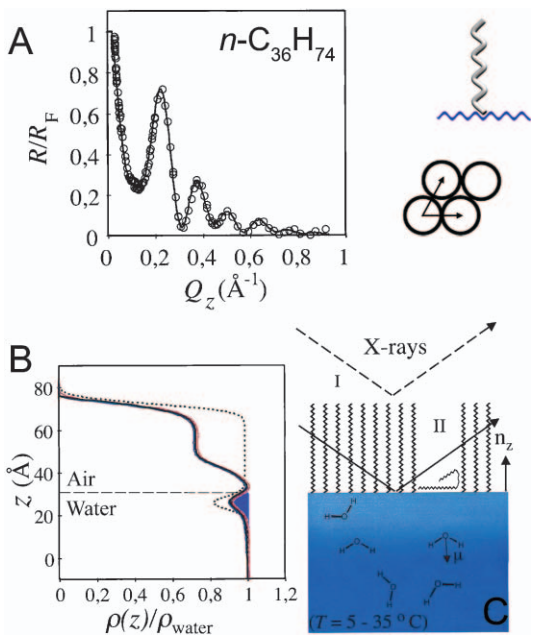

Fig. 4 A: X-ray reflectivity of a paraffin monolayer on water and the hexagonal unit cell. B: Experimental (solid line, zone I + II) and modelled electron density (dotted line, zone I) corresponding to the data shown in A. C: Schematic illustration of the experimental results. (From ref. 22).

Critical fluctuations in phospholipids

The addition of a polar headgroup to a long-chain alkane (*e.g.* paraffin) yields a classical amphiphile. Phospholipids are well-known examples of such relatively simple amphiphilic molecules, since they hold an essential function in biology as the molecular backbone of cellular membranes. Although the biological phospholipid membrane is essentially a double layer, Langmuir films of different phospholipids have been employed as model systems for the cellular lipid bilayer due to the simplicity and controllability of such planar interfacial monolayers.[25]

In contrast to the static polycrystalline paraffin monolayers described above, Langmuir films of phospholipids are relatively dynamic. At 12 °C Langmuir films of the zwitterionic phospholipid dimyristoyl phosphatidylcholine (DMPC) demonstrate a phase transition between a fluid-like *liquid-expanded* (LE) and a solid *liquid-condensed* (LC) phase, which can be seen as a horizontal plateau in the *Π*–A isotherm (Fig. 5). The length of this plateau marks the coexistence region of the LE and LC phases, where the latter appears as domains in a matrix of the LE phase.

At elevated temperatures, the coexistence region gradually becomes narrower until the critical temperature is reached at 20 °C. Close to this point, strong fluctuations appear in the size of the monolayer domains, indicating that no characteristic length scale is present—a phenomenon known as critical

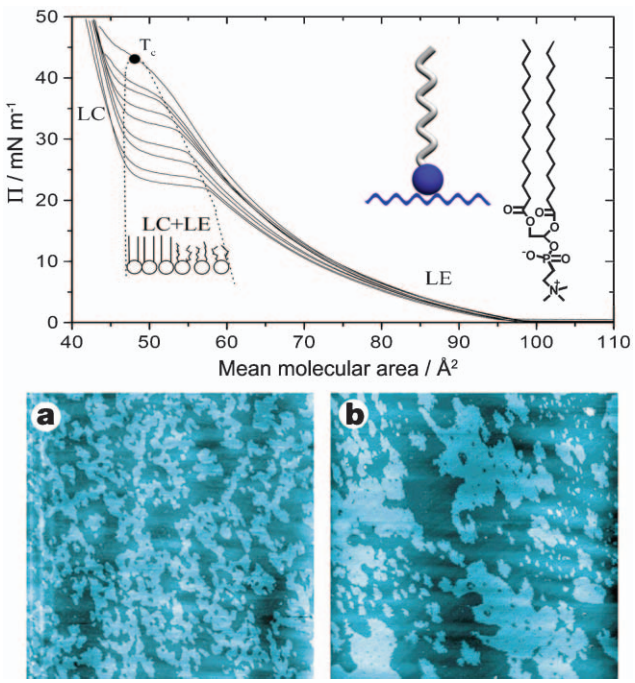

Fig. 5 Top: Isotherms of dimyristoyl phosphatidylcholine (DMPC) at temperatures ranging from 12–20 °C. Bottom: AFM images showing critical fluctuations in phospholipid monolayers for a) DMPC (25 × 25 μm²) and b) dipalmitoyl phosphatidylcholine (DPPC) (20 × 20 μm²) at their respective critical points. Adapted from ref. 25.

fluctuations. These fluctuations occur on every scale, from the single molecular level to the entire system.

Fig. 5a,b shows AFM images of two different phospholipid monolayers close to their respective critical points. The Langmuir monolayers have been immobilized by horizontal LB-transfer onto hydrophilic mica.[25] The high areas (light) represent the LC phases and the lower (darker) areas correspond to the LE phase. The height difference between the light and dark areas is about 5 Å. This phase behavior has recently been used as a template to structure molecular electronic building blocks[26,27] (*vide infra*).

Simple electroactive amphiphiles

With the aim of designing self-assembling electronically conductive molecular systems it soon becomes evident that exceedingly more complex molecules than paraffin or phospholipids need to be employed. Amphiphilic molecules comprising an electro-active head group attached to an alkyl-chain tail is an attractive first approach for the introduction of a functional moiety into Langmuir monolayers.[28] As an example of such a molecule, structural studies of the electron acceptor 2-octadecylsulfanyl-*p*-benzoquinone (Fig. 6) were performed on it both as a floating monolayer on water and as a bilayer transferred to a solid substrate by the LB-technique.[29]

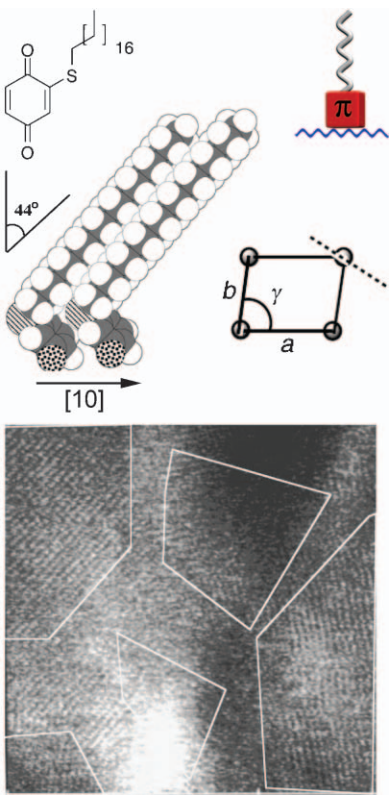

Fig. 6 Top: Chemical structure of 2-octadecylsulfanyl-*p*-benzoquinone, a model of two adjacent molecules in a Langmuir film and the unit cell including tilt direction (dotted line). Bottom: AFM image (31×31 nm^2) of a double layer of the above molecule. The white lines correspond to highly ordered domains. From ref. 29.

Because such functionalised molecules often have relatively large head groups compared to the alkyl tails, an understanding of the packing properties of molecules with a 'cross-sectional mismatch' between head and tail groups is required.

The X-ray scattering from a densely packed monolayer reveals three distinct diffraction peaks corresponding to an oblique unit cell with an area of 23.1 Å^2 (Fig. 6). This area is very close to the projected area of the head group, which is thus forced into a close-packed arrangement, whereas the alkyl chain only needs $\approx$19 Å^2 in its upright position, and therefore maximizes the intermolecular packing of neighboring chains by tilting.

AFM investigations of LB-transferred bilayers (Fig. 6) reveal that the film contains ordered domains separated by several nanometers wide domain boundaries. Fourier analysis of the crystalline domains yields very accurate unit cell parameters, which are listed in Table 1. A comparison of the unit cell parameters obtained with GIXD and AFM respectively shows that LB-transferred films of 2-octadecylsulfanyl-*p*-benzoquinone expand by roughly 17% during the transfer process. The head groups are thus no longer close packed in the transferred films, which indicates that the molecules relax towards a more thermodynamically favorable structure once transferred. A major part of the cohesive energy in monolayers of this molecule is associated with the alkyl-chains, and they therefore become a decisive factor in the competition between the packing of head and tail groups when the barrier pressure on the film is released in the LB-transfer process. The wide domain boundaries observed are likely to be caused by the high degree of tilting of the alkyl-chains. As a result, adjacent crystalline domains are isolated from each other. These issues hinder the realisation of highly conducting LB-films of 2-octadecylsulfanyl-*p*-benzoquinone, since this would require good electronic contact between the head groups all the way from a source to a drain electrode, as well as no—or only very narrow—domain boundaries between these electrodes.

Amphiphilic polythiophene

In an attempt to overcome some of the shortcomings of the simple electroactive amphiphiles in relation to the fabrication of conducting monomolecular films, attention was turned towards π-conjugated polymers. By covalently linking the individual electroactive moieties into a continuous polymer the electronic contact between neighbouring headgroups would increase considerably and allow an extended π-conjugated system to develop in one direction. In addition, face-to-face π–π-stacking of adjacent polymer chains would also allow electronic contact perpendicular to the chain direction.

By design and synthesis of regioregular head-to-tail coupled amphiphilic polythiophene copolymers, incorporating a

Table 1 Lattice parameters for Langmuir and Langmuir–Blodgett films of 2-octadecylsulfanyl-*p*-benzoquinone

Parameter	Langmuir film	LB-film
a/Å	5.60	5.87
b/Å	4.19	4.56
γ/°	80	82.3
Area/Å^2	23.1	26.5

This journal is © The Royal Society of Chemistry 2005

hydrophobic group at the 3-position of one thiophene and a hydrophilic group at the 3′-position of the adjacent thiophene (Fig. 7A) well defined Langmuir and LB-films have been prepared and processed on the nanometer scale.[30,31] These polymers form a rigid board-like structure that has a hydrophobic side and a hydrophilic side (*i.e.* a "Janus"-type structure[32]) with the highly conjugated polythiophene backbone as the functional element. When spread at the air/water interface the hydrophilic side interacts with the subphase and the hydrophobic side points away from the water surface in an adapted amphiphilic structure, while maintaining the preferred transoid conformation of the thiophene backbone. This self-assembly process at the air/water interface ultimately leads to the formation of highly ordered crystalline domains as revealed by GIXD studies.[30,31] The diffraction pattern corresponds to the two-dimensional unit cell shown in Fig. 7B. Since only every second thiophene unit contains an alkyl substituent, neighboring polymers can dock onto each other by a displacement of one thiophene unit along the polymer backbone, which results in a close-packed π-stacked structure. Hence, the π-stacking of neighboring polymer chains dominates the overall packing structure of the Langmuir films.

From the diffraction peak widths it was possible to determine the size of the coherent scattering domains. This corresponded to roughly 13 parallel π-stacked polymer chains. The complete self-assembly process of the amphiphilic polythiophenes, from solution to ordered crystalline domains, is illustrated schematically in Fig. 8.

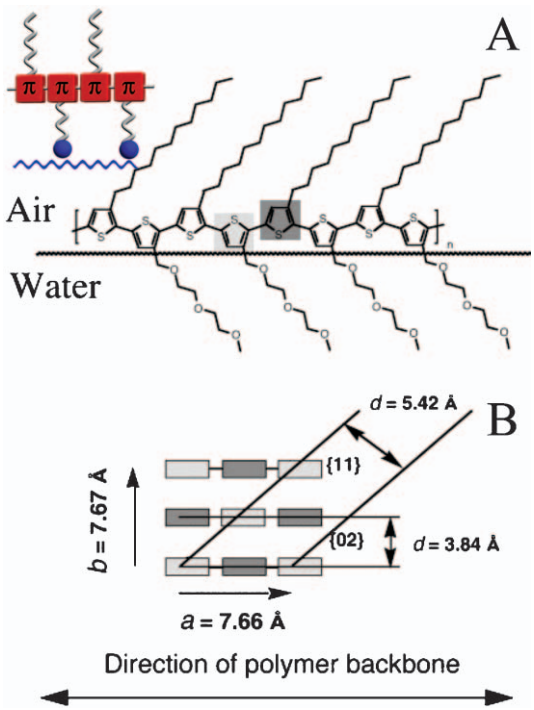

Fig. 7 A: Side view of the amphiphilic polythiophene organized on a water surface. B: Top view of the monolayer packing, showing thiophene units (grey boxes) in a centered rectangular unit cell. Adapted from ref. 10.

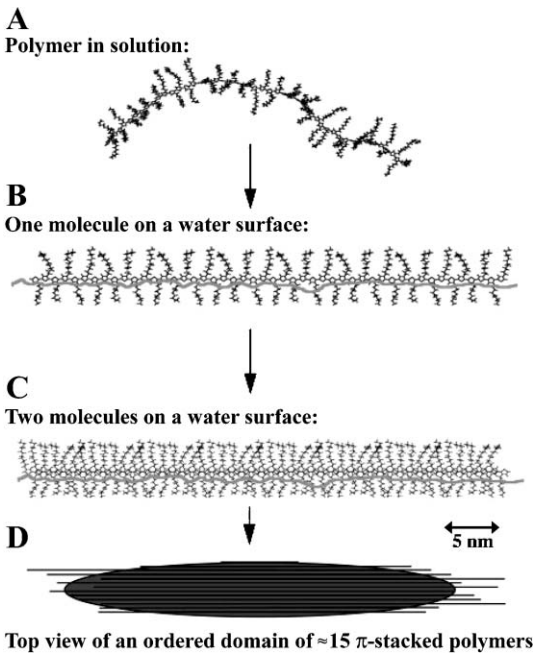

Fig. 8 Summary of the self-assembly process of the amphiphilic polythiophene derivatives on the water surface. A–C: Side views. D: Top view. From ref. 10.

Very high conductivities in excess of 100 S cm^{-1} have been reported for microscale domains in doped amphiphilic polythiophene monolayer films.[33]

Polycyclic aromatic hydrocarbons

The syntheses of a remarkable number of well-defined large polyaromatic hydrocarbons (PAHs) have been performed by Müllen *et al.*[34,35] The synthetic routes facilitate a systematic control of the size and shape of the PAHs, and furthermore allow the attachment of functionalized substituents to the periphery of the polyaromatic core. Hexa-*peri*-hexabenzocoronenes (HBCs) constitute a subclass of these PAHs, which consist of thirteen fused benzene rings in a planar, disk-like arrangement (Scheme 1). Hexa-alkane substituted HBCs are known to form discotic liquid crystalline phases[36] and quasi one-dimensional columnar aggregates, which show very high charge carrier mobilities along the stacking direction.[37] Furthermore, the alkyl side-chains facilitate an increased solubility in common organic solvents.

A series of amphiphilic HBCs was studied, which contained five hydrophobic alkyl substituents (branched or straight-chain) in addition to one polar side chain at the periphery of the planar graphene core, as shown in Scheme 1. All of these amphiphilic HBC derivatives formed well-behaved monolayers on water.[38,39]

For the straight-chain *n*-dodecyl substituted molecule (Scheme 1, **1a**) GIXD studies showed that the structure of Langmuir monolayers is governed by a competition between hexagonal packing of the alkyl side-chains and π-stacking of the polyaromatic cores.[39] This competition gives rise to two distinct phases in the monolayers. When spread from solution, and in the absence of external pressure, the molecules

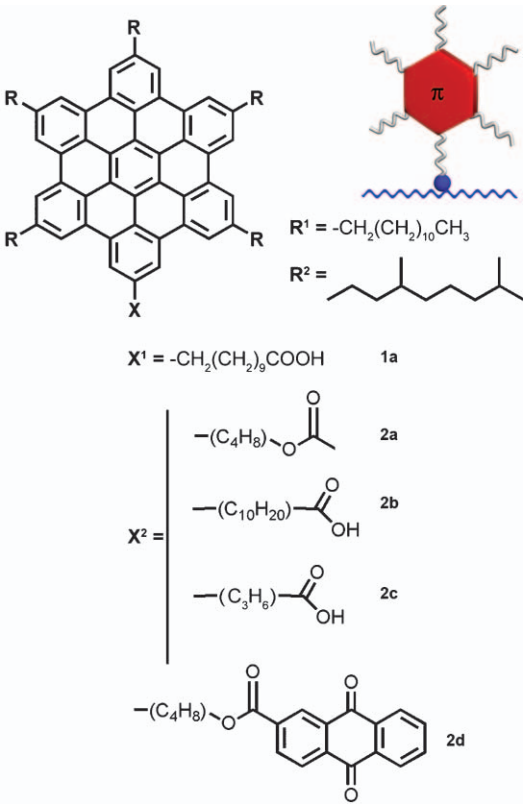

Scheme 1 Structure of amphiphilic hexabenzocoronenes studied at the air/water interface. (Ref. 38,39).

spontaneously self-assemble into lamellae on the water surface. In this *low-pressure* phase the π-stacks are tilted and rotated in the direction of the lamellae. In this case, the π-stacking of the HBC cores holds a very high coherent order, leading to the formation of a rather delocalized electronic band structure in the one-dimensional columns. Application of a lateral pressure, by use of the Langmuir trough barriers, forces the monolayer film into another phase in which the alkyl chains are crystalline and the coherence in the π-stack is lost, thus localizing the electrons on the individual HBCs. This results in a measurable change in the electronic properties of the film (Fig. 9) as revealed by Kelvin force microscopy.[39]

Replacing the straight side-chains with branched chains (Scheme 1, **2a–d**) resulted in less crystalline and more flexible materials, which were better suited for multilayer formation *via* the LB-technique.[38] The packing of these less crystalline HBCs was dominated entirely by the π–π stacking of the polyaromatic cores.

Oligo(*p*-phenylenevinylene)

A common structural feature of the studied molecules thus far, has been the presence of at least one alkyl-chain. However, packing studies of π-conjugated molecules without alkyl-substituents have also been performed using thiol end-capped oligo(*p*-phenylenevinylene)s (OPVs, Fig. 10). When deprotected, the thiol end-groups can attach to gold surfaces, due to the strong sulfur–gold interactions (*vide infra*).

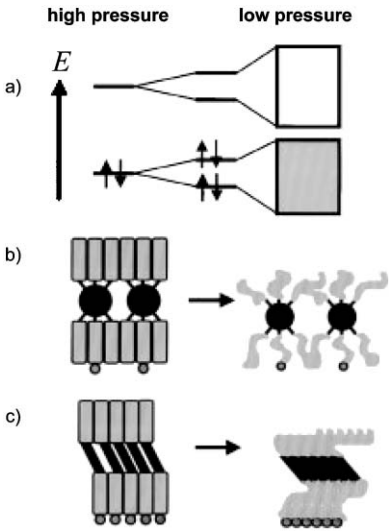

Fig. 9 Schematic drawing of the transformation from the high- to low-pressure phase. a) The electronic structure changes caused by delocalization of the localized HBC states as the pressure is decreased. b) View along the lamellae (end view). The alkyl chains are closely packed in the high-pressure phase and disordered in the low-pressure phase. c) Side view of a lamella of the high-pressure phase (left) and low-pressure phase (right). In the low-pressure phase a close π–π contact is obtained. From ref. 39.

The OPV molecules spontaneously form highly crystalline films when spread on a water surface.[40,41] The GIXD measurements reveal a series of sharp Bragg peaks in the region Q_{xy} = 1.1–2.0 Å^{-1} (Fig. 10) with an in-plane coherence length around 550 Å. The absence of alkyl-substituents thus

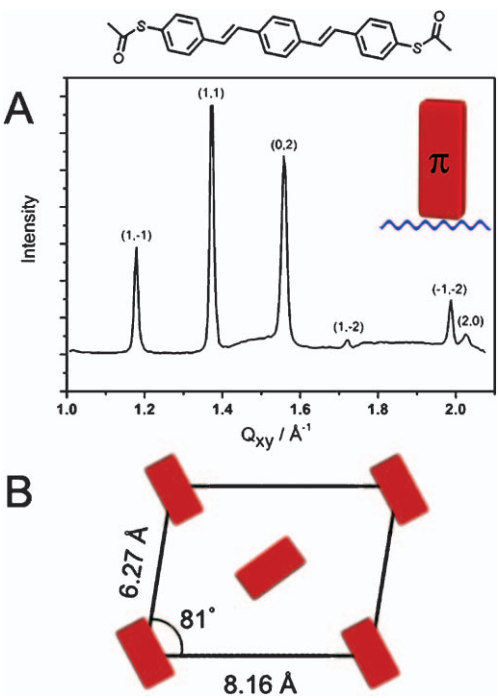

Fig. 10 Acetyl-protected thiol end-capped oligo(*p*-phenylenevinylene). A: GIXD data. B: Schematic illustration of the unit cell (top view).

This journal is © The Royal Society of Chemistry 2005

facilitates a very well-ordered packing arrangement of the electroactive π-conjugated moieties. The OPV molecules are oriented with their long molecular axis normal to the water surface, as shown in the two-dimensional unit cell (Fig. 10B). X-ray reflectivity measurements established that Langmuir films of the OPV molecule spontaneously formed partial double layer structures on water.

Summary of the structural studies

The air/water interface is an ideal model system for studies of supramolecular self-assembly in two dimensions. When cast on water, molecular building blocks are transferred from a disordered state in solution into more or less well-ordered structures in a Langmuir film. The resulting supramolecular arrangement can be probed *in-situ* with sub-nanometer resolution using surface sensitive X-ray scattering, and the nano- and micro-scale structures of substrate transferred films can be examined with scanning probe techniques. In the long term such systematic structural studies are necessary to relate molecular properties to device performance in a rational way.

The collective properties of organic supramolecular assemblies depend crucially on their organization. As an example, high electronic charge carrier mobility requires a very high degree of local molecular order. At the same time, the material should be uniform at a macroscopic scale, in order to eliminate the influence of defects and domain boundaries, which will otherwise cause a decrease in the overall charge carrier mobility. Electroactive organic molecules typically incorporate π-conjugated moieties, which can stack to form highly ordered local packing arrangements. This is exemplified by the high crystallinity observed in Langmuir films of oligo(*p*-phenylene-vinylene)s. The addition of one or more alkyl-substituents to the conjugated π-electron system tremendously increases the overall solubility—and thus processability—of the molecules. However, this added flexibility also leads to a competition between different structural motifs dominated by either the packing of alkyl-chains (*e.g.* the simple electroactive amphiphile) or the π-system (*e.g.* the amphiphilic polythiophenes). In special cases, the packing can to some extent be regulated by the pressure exerted by the Langmuir trough barriers, as shown for Langmuir monolayers of the hexa-*peri*-hexabenzocoronenes.

Self-assembly of electronic thin films and circuitry on water

Au nanoparticles

Thus far the focus has been aimed exclusively at organic molecules as building blocks for supramolecular assemblies. However, another attractive and versatile building block for nanoscale architectures is offered by inorganic metal nanoparticles with a diameter < 5 nm covered by a self-assembled monolayer of organic ligands.[42] Such ligand-stabilized nanoparticles can be considered as ordinary molecular compounds, the chemistry of which is governed largely by the nature of the ligand shell, whereas the size-dependent electronic and optical properties are determined primarily by the metallic core. The physical properties can be regarded as intermediate between atomic and bulk properties due to quantum size effects in these small particles. A particularly interesting example of quantum confinement in small metal nanoparticles is the observation of Coulomb blockades,[43] indicative of single electron transitions. This occurs if the electrostatic energy $E_{el} = e^2/2C$ is larger than the thermal energy $E_T = k_B T$. In this case, tunnelling of a single electron onto the particle prevents the transfer of a second electron due to Coulomb repulsion. The capacitance, C, decreases with decreasing particle size, consequently metal nanoparticles in the 1–2 nanometer range are required for the observation of single electron effects at room temperature.[43]

We have studied the self-organization process of a series of alkanethiolate stabilized gold nanoparticles with a core diameter of 1.6 nm at the air/water interface.[44] Different end-group functionality (hydrophilic or hydrophobic) and/or length of alkanethiolates were introduced into the ligand shell by a ligand place-exchange procedure in solution.[45] GIXD investigations of the nanoparticle monolayers on water confirmed the well-known hexagonal close-packing of the particles (Fig. 11A). A combination of these in-plane data with AFM height imaging on LB-transferred monolayers showed that nanoparticles with a hybrid hydrophilic/hydrophobic ligand shell respond to the asymmetric environment imposed by the water surface by adapting to an amphiphilic distribution of ligands on the nanoparticle core. This adaptive nature is facilitated by the mobility of the ligands on the particle surface[46–48] as illustrated in Fig. 11B.

Electronic transport measurements at the nanoscale

The self-assembled monolayers of electroactive molecules can be regarded as model systems for three-dimensional bulk materials or thin films since many of these (*e.g.* polythiophenes and HBCs) organize in layered structures similar to

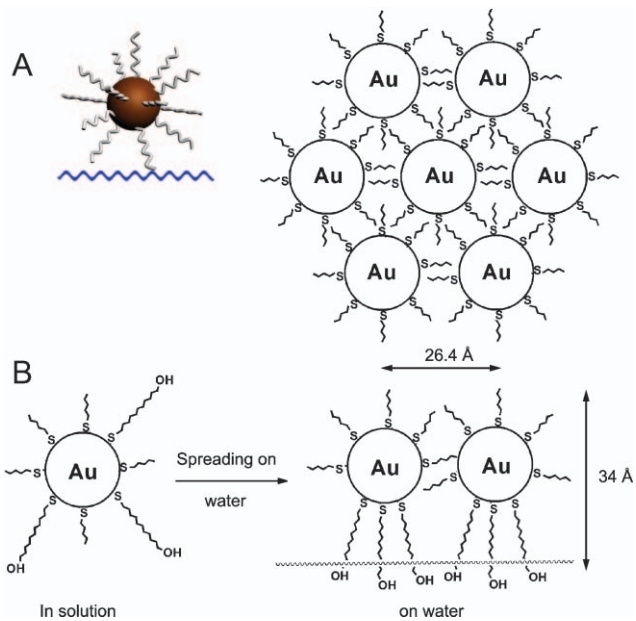

Fig. 11 Schematic illustration of the amphiphilic reorganization of the ligand shell of mixed long-chain hydrophilic and short-chain hydrophobic nanoparticles when spread at the air/water interface. A: Top view of the hexagonal lattice. B: Side view.

Langmuir–Blodgett films.[49] Langmuir–Blodgett films have the advantage that they allow the scale dependence of the electronic properties to be elucidated by surface sensitive techniques. Such investigations, exemplified below, uncover the generic complexity of the hierarchical morphology of bulk materials, thin film, or Langmuir film, arising due to the polycrystalline nature of the sample. These issues hinder a direct correlation between the measured conductivity on a macroscopic scale and the nanoscale structure. Consequently, methods to investigate the nanoscale transport properties need to be developed. Thus far, certain types of AFM modifications present some of the few possibilities for this purpose. One example is the Kelvin Force AFM,[50] which maps out the electrochemical potential of a surface with nanometer resolution. This is illustrated in Fig. 12A, which shows a Kelvin Force AFM scan of a doped monolayer of amphiphilic polythiophene (*cf.* Figs. 7–8) transferred to a substrate containing an electrode system.[51] The bottom profile shows the topography of the monolayer-covered substrate, while the top profile shows the potential landscape with an externally applied bias of 0.5 V between the electrodes. The electrodes dominate the topography image, as they protrude approximately 50 nm above the surface. The potential profile clearly shows the potential drop between the electrodes. Fig. 12B shows a single scan line from the KFM measurement, which represents a voltage profile from one electrode to the other. The profile reveals a series of step-like features, which are related to the electronic domain structures within the sample.[51] The flat parts of the profile correspond to close-packed domains of π-stacked polymers, which have a very high local conductivity. The potential drops are associated with the domain boundaries within the monolayer, which are thus characterized by low conductivity.

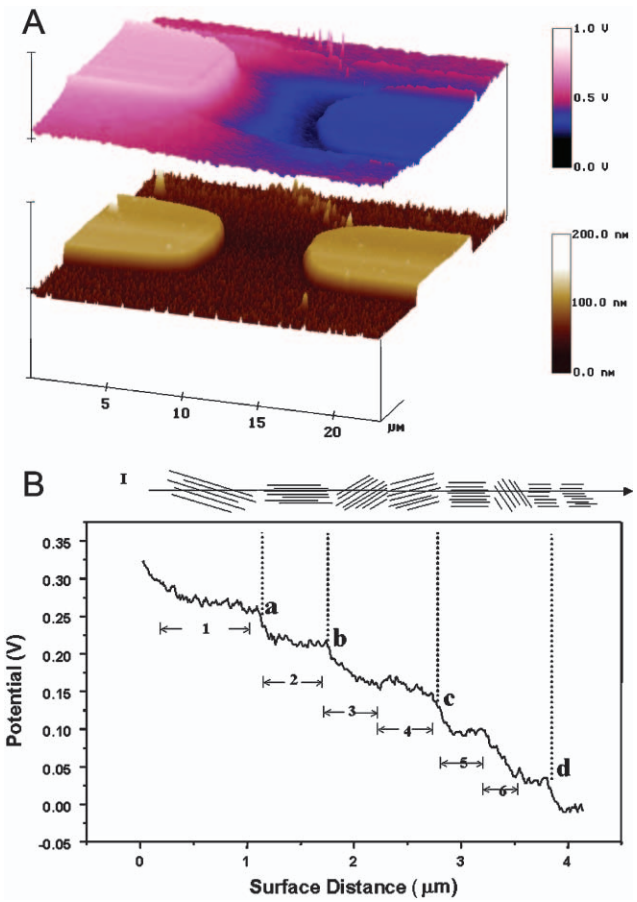

Fig. 12 A: KFM measurement on a monolayer of amphiphilic polythiophene covering a substrate, which contains an electrode system. The bottom 3D profile shows the topography of the sample, and the top 3D profile shows the potential landscape in the same region with an externally applied voltage of 0.5 V. B: A single scan line from the KFM data. From ref. 51.

Conducting probe atomic force microscopy (CPAFM) is another AFM modification, which can be used to study electronic transport characteristics at the nanoscale. The method was developed by Frisbie *et al.*[52] and uses a gold coated tip as one electrode to do point contact electrical measurements combined with *in-situ* switching to tapping mode AFM imaging. CPAFM is useful for electrical transport characterizations of small organic structures and thin films. Depending on the geometrical placement of the second electrode, transport can be probed either perpendicular or parallel to the substrate.

Self-assembled circuitry

While the hexagonal close-packed lattice of ligand-stabilized nanoparticles (Fig. 11A) has interesting implications for the fabrication of extended two-dimensional systems,[53] the focus of much current interest revolves around the fabrication of nanostructured one- and zero-dimensional materials.

In an attempt to break-up the hexagonal lattice of the nanoparticles we have investigated the use of phase separation phenomena to nanopattern the assembly of particles on water.

In a series of experiments, alkanethiolate protected gold nanoparticles and the phospholipid DPPC (*cf.* Fig. 5) were co-spread from the same solution onto a pure water surface at various temperatures and surface compositions.[26] The resulting monolayers were transferred at different surface pressures onto freshly cleaved mica for AFM investigations or onto amorphous carbon for TEM imaging. In a typical experiment, the surface area covered with nanoparticles was around 10% for fully compressed films. The AFM investigations (Fig. 13) revealed that at low pressure, the gold nanoparticles were dissolved in the LE phase of the phospholipid (Fig. 13A), whereas at pressures beyond the coexistence region the

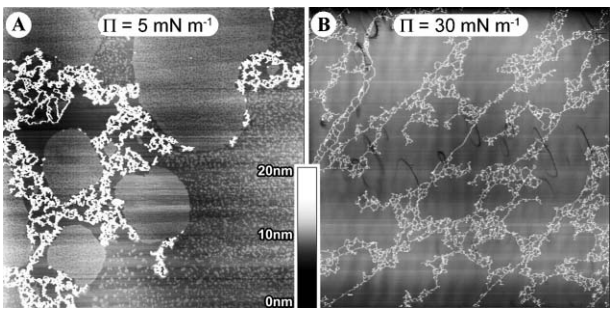

Fig. 13 AFM images (50 × 50 μm^2) of LB-films of DPPC and dodecanethiolate covered gold nanoparticles (10% by area) transferred at A) 5 mN m^{-1} and B) 30 mN m^{-1}. Adapted from ref. 26.

This journal is © The Royal Society of Chemistry 2005

nanoparticles were decorating the phase boundaries of the LC domains (Fig. 13B). TEM inspection additionally showed that the nanoparticles sintered into continuous quasi one-dimensional maze-like wire structures as shown in Fig. 14A. The width of these wires corresponded to the diameter of one nanoparticle (< 3 nm), whereas the length of the wires typically extended over several tens of nanometers. The gaps between adjacent wire-segments could be tuned by changing the length of the alkanethiolate ligands on the nanoparticles, and thus varied between ≈1.7–3 nm.

These intricate, yet intriguing self-assembled structures can be likened, at least visually, to the circuitry of modern day microelectronics—although at a much smaller length scale. The continuous wires of gold, only a few nanometers in width, represent a notable decrease in size as compared to even the smallest features of mass-produced electronic circuitry.

The wire-structures could be used as a template for the self-assembly of functional organic molecules, and—through bridging of individual wire-segments—the fabrication of an extended interconnected network.[27] A π-conjugated organic oligomer of the type shown in Fig. 14C was chosen as the linker (*i.e.* thiol end-capped oligo-*p*-phenylenevinylenes, OPVs[54,55]).

The LB-technique was used to transfer the gold-wire network onto a solid support, which contained a set of prefabricated gold electrodes prepared by UV/e-beam lithography. Each of these electrodes could be connected to external wiring and thus used as a static electrode in CPAFM transport measurements[52] or a bias voltage could be applied between two electrodes (Fig. 14B). Addition of the organic linkers was done by exposing the above sample to a solution of the OPV molecules, which had been deprotected by ethylenediamine to expose the free thiol end-group. This procedure was done in argon flushed solutions in order to prevent the polymerization of individual OPVs. The conductivity of a gold-wire network without OPV molecules was lower than 0.05 S m^{-1}. This value increased to around 18 S m^{-1} for OPV treated networks, where the OPV molecules were long enough to bridge the gap between neighboring wire segments (Fig. 15). For OPV molecules too short to bridge the gap between wires or for longer wire separations the conductivities were in the range 0.4–1.5 S m^{-1}. The average single molecule conductance was estimated to G ≈ 20 MΩ for molecules, which are covalently bound to both sides of the gap.[27]

Single molecule measurements

The electronic measurements described above address an ensemble of molecules, from which certain averaged values for single molecules can be deduced. Recently, however, a few examples of direct electronic characterization of single molecules have emerged, employing both two-terminal[56–59] and three-terminal devices.[60–62] One example is a three-terminal single electron transistor (SET) device incorporating a single *p*-phenylenevinylene oligomer sandwiched between two electrodes in the vicinity of a gate-electrode[62] (Fig. 16A). The electronic transport properties of the molecule were measured at 4 K. By varying the gate voltage, V_g, of the SET

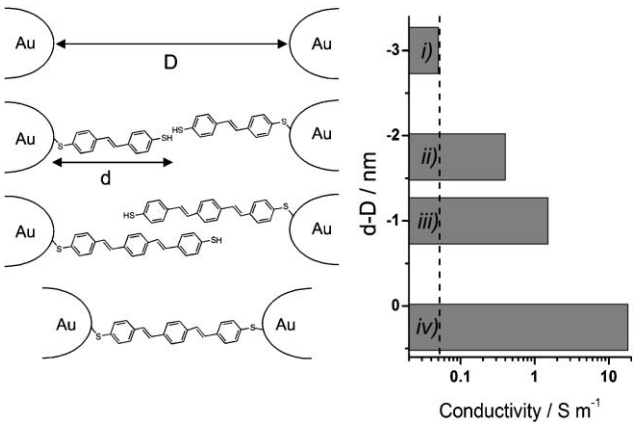

Fig. 15 Left: Schematic representation of the average gap-size (D) between neighboring gold-wire segments compared to the length of the OPV molecule (d) shown for four different molecular geometries. Right: Measured conductivities *vs.* d-D corresponding to the different geometries. The vertical dashed line marks the detection limit of the experimental setup. Adapted from ref. 27.

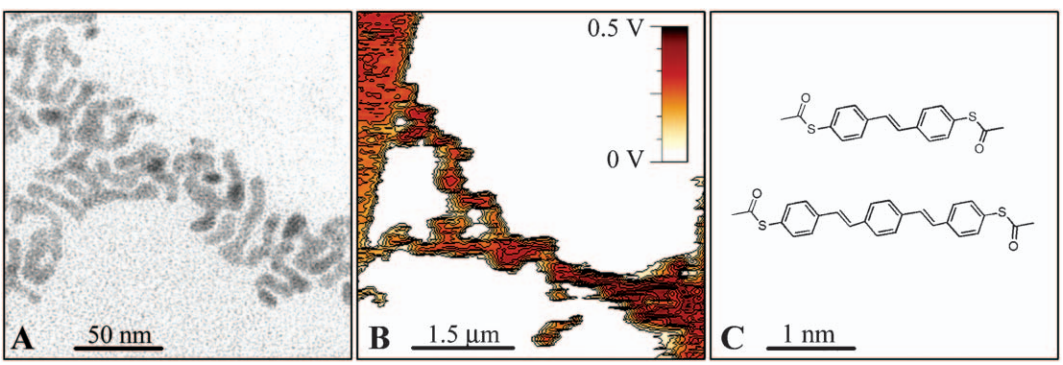

Fig. 14 A) High resolution TEM image gold-wire segments in a matrix of phospholipid transferred at 30 mN m^{-1}. The smallest spacings between wire segments were measured from the TEM image to be 3.0 nm for dodecanethiolate covered particles and 1.7 nm for pentanethiolate covered particles. B) Kelvin force microscope (KFM) image of a network of molecularly linked gold nanowires. The nonconducting phospholipids molecules constitute the white background. A potential of 0.5 V is applied to two prefabricated electrodes (top left and bottom right of image). C) Thiol end-capped OPV molecules used in the experiments. The S–S′ distance was estimated to 1.3 and 1.9 nm respectively using semiempirical PM3 calculations. From ref. 27.

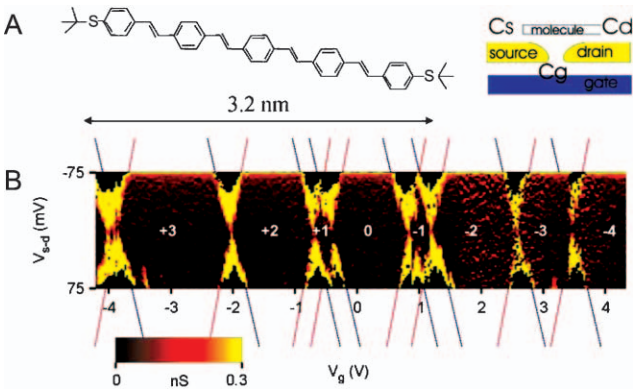

Fig. 16 Single molecule transistor device. A: Molecular structure of the oligomer and schematic illustration of the experimental setup. B: Experimental results showing the differential conductance ($dI_{s\text{-}d}/dV_{s\text{-}d}$) for nine distinct redox-states as a function of $V_{s\text{-}d}$ and V_g (white numbers denote the charge on the molecule). Adapted from ref. 62.

device in small steps, several redox-states of the molecule could be probed. The source-drain current–voltage characteristics ($I_{s\text{-}d}$; $V_{s\text{-}d}$) were measured at each step, as illustrated in Fig. 16B, where the differential conductance, $dI_{s\text{-}d}/dV_{s\text{-}d}$, is plotted (in colour code) as a function of the gate voltage, V_g, and the source-drain voltage, $V_{s\text{-}d}$. The light areas in Fig. 16B represent transmitting (open) states of the device, whereas the dark diamonds correspond to regions of zero current.

For the first time, this type of measurement allows the relation between "redox-chemistry" and "transistor characteristics" to be studied at the single molecule level, and it has already uncovered important new insights into the nature of the contact region between the molecule and the electrodes. In this case, in particular about the role of image charges.

Outlook

The successful realization of molecular based electronics as a future successor to modern day microelectronics requires an unprecedented level of understanding regarding the fundamental properties of individual molecules, ensembles of molecules as well as their incorporation into electrode systems.

The emerging insight stemming from single molecule measurements combined with the steady progress in the design and preparation of self-assembled systems may eventually lead to actual electronic circuitry fabricated from the "bottom-up".

As an embryonic example of such a strategy, one may imagine the fabrication of neuromorphic network architectures[63,64] based on the surfactant-templated self-assembly of nanoparticles at the air/water interface, similar to the procedure described above (Figs. 13–14). These percolation networks of sintered nanoparticles can be controlled and manipulated by purely chemical methods, *e.g.* by changing the templating surfactant or by varying the chemical nature of the nanoparticle ligand shell. Furthermore, the self-assembled nanowire structures provide a scaffold for the attachment of two- or three-terminal functional molecules, thereby facilitating the formation of an integrated circuit of self-assembled nanodevices. Future developments may combine such self-assembled neuromorphic networks with a "top-down" lithographically fabricated electrode system into a hybrid semiconductor/nanodevice integrated circuit (Fig. 17). The electrode system provides a way to electronically address the neuromorphic network, which could respond in many different ways to different combinations of potentials applied to the external electrodes.

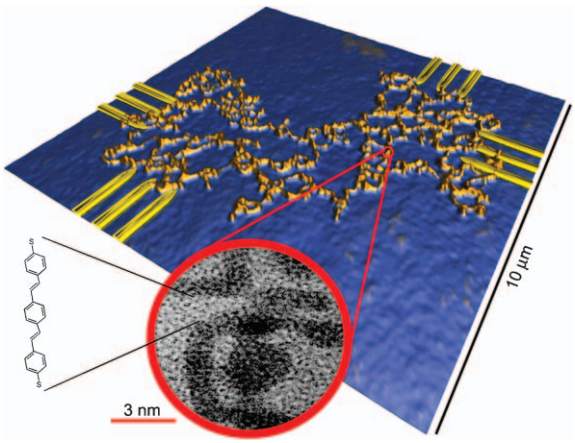

Fig. 17 Putative hybrid semiconductor/nanodevice integrated circuit, consisting of a neuromorphic network architecture of nanoparticles, which have been self-assembled on water and transferred to an electrode system. The percolation network is a real AFM topography image[26] and the inset shows a TEM micrograph of the sintered nanoparticles. The electrodes have been added graphically for illustrative purposes.

Acknowledgements

Support from the Danish research councils and the EU is gratefully acknowledged.

Kasper Nørgaard and Thomas Bjørnholm*
Nano-Science Center, Department of Chemistry, University of Copenhagen, Universitetsparken 5, DK-2100, Copenhagen Ø, Denmark. E-mail: tb@nano.ku.dk; Fax: +45 3532 0460; Tel: +45 3532 1835

Notes and references

1 J.-M. Lehn, *Pure Appl. Chem.*, 1978, **50**, 871.
2 A. Gavezzotti, *Acc. Chem. Res.*, 1994, **27**, 309–314.
3 G. R. Desiraju, *Curr. Opin. Solid State Mater. Sci.*, 1997, **2**, 451–454.
4 J. H. Burroughes, D. D. C. Bradley, A. R. Brown, R. N. Marks, K. Mackay, R. H. Friend, P. L. Burns and A. B. Holmes, *Nature*, 1990, **347**, 539–541.
5 J. H. Burroughes, C. A. Jones and R. H. Friend, *Nature*, 1988, **335**, 137–141.
6 G. Yu, J. Gao, J. C. Hummelen, F. Wudl and A. J. Heeger, *Science*, 1995, **270**, 1789–1791.
7 *Chem. Mater.*, 2004, **16**, special issue on organic electronics.
8 H. Shirakawa, E. J. Louis, A. G. MacDiarmid, C. K. Chiang and A. J. Heeger, *J. Chem. Soc., Chem. Commun.*, 1977, 578–580.
9 D. Jerome, A. Mazaud, M. Ribault and K. Bechgaard, *J. Phys. Lett.*, 1980, **41**, L91.
10 T. Bjørnholm, T. Hassenkam and N. Reitzel, *J. Mater. Chem.*, 1999, **9**, 1975–1990.
11 I. Langmuir, *J. Am. Chem. Soc.*, 1917, **39**, 1848.
12 K. B. Blodgett, *J. Am. Chem. Soc.*, 1935, **57**, 1007.
13 I. Langmuir and V. J. Schaefer, *J. Am. Chem. Soc.*, 1938, **60**, 1351.
14 J. Als-Nielsen, D. Jacquemain, K. Kjaer, F. Leveiller, M. Lahav and L. Leiserowitz, *Phys. Rep.*, 1994, **246**, 251.

 This journal is © The Royal Society of Chemistry 2005

15 K. Kjaer, *Physica B*, 1994, **198**, 100.
16 T. R. Jensen and K. Kjaer, in *Novel Methods to Study Interfacial Layers*, ed. D. Möbius and R. Miller, Elsevier, Amsterdam, 2001, p. 205.
17 G. Binnig, C. F. Quate and C. Gerber, *Phys. Rev. Lett.*, 1986, **56**, 930.
18 J. S. Pedersen and I. W. Hamley, *J. Appl. Crystallogr.*, 1994, **27**, 36.
19 W. Blokzijl and J. B. F. N. Engberts, *Angew. Chem.*, 1993, **32**, 1545–1579.
20 P. Ball, *Nature*, 2003, **423**, 25–26.
21 F. H. Stillinger, *J. Solution Chem.*, 1973, **2**, 141.
22 T. R. Jensen, M. O. Jensen, N. Reitzel, K. Balashev, G. H. Peters, K. Kjaer and T. Bjørnholm, *Phys. Rev. Lett.*, 2003, **90**, 86101.
23 M. Li, A. A. Acero, Z. Huang and S. A. Rice, *Nature*, 1994, **367**, 151.
24 S. P. Weinbach, I. Weissbuch, K. Kjaer, W. G. Bouwman, J. Als-Nielsen, M. Lahav and L. Leiserowitz, *Adv. Mater.*, 1995, **7**, 857.
25 L. K. Nielsen, T. Bjørnholm and O. G. Mouritsen, *Nature*, 2000, **404**, 352.
26 T. Hassenkam, K. Nørgaard, L. Iversen, C. J. Kiely, M. Brust and T. Bjørnholm, *Adv. Mater.*, 2002, **14**, 1126–1130.
27 T. Hassenkam, K. Moth-Poulsen, N. Stuhr-Hansen, K. Nørgaard, M. S. Kabir and T. Bjørnholm, *Nano Lett.*, 2004, **4**, 19–22.
28 M. R. Bryce and M. C. Petty, *Nature*, 1995, **374**, 771.
29 J. Garnaes, N. B. Larsen, T. Bjørnholm, M. Jørgensen, K. Kjaer, J. Als-Nielsen, J. F. Jørgensen and J. A. Zasadzinski, *Science*, 1994, **264**, 1301.
30 T. Bjørnholm, D. R. Greve, N. Reitzel, T. Hassenkam, K. Kjaer, P. B. Howes, N. B. Larsen, J. Bøgelund, M. Jayaraman, P. C. Ewbank and R. D. McCullough, *J. Am. Chem. Soc.*, 1998, **120**, 7643.
31 N. Reitzel, D. R. Greve, K. Kjaer, P. B. Howes, M. Jayaraman, S. Savoy, R. D. McCullough, J. T. McDevitt and T. Bjørnholm, *J. Am. Chem. Soc.*, 2000, **122**, 5788.
32 A. Marsh, E. G. Nolen, K. M. Gardinier and J.-M. Lehn, *Tetrahedron Lett.*, 1994, 397–400.
33 P. Bøggild, F. Grey, T. Hassenkam, D. R. Greve and T. Bjørnholm, *Adv. Mater.*, 2000, **12**, 947–950.
34 M. D. Watson, A. Fechtenkötter and K. Müllen, *Chem. Rev.*, 2001, **101**, 1267–1300.
35 M. Müller, C. Kübel and K. Müllen, *Chem. Eur. J.*, 1998, **8**, 2099–2109.
36 P. Herwig, C. W. Kayser, K. Müllen and H. W. Spiess, *Adv. Mater.*, 1996, **8**, 510–513.
37 A. M. van de Craats, J. M. Warman, A. Fechtenkotter, J. D. Brand, M. A. Harbison and K. Müllen, *Adv. Mater.*, 1999, **11**, 1469–1472.
38 B. W. Laursen, K. Nørgaard, N. Reitzel, J. B. Simonsen, C. B. Nielsen, J. Als-Nielsen, T. Bjørnholm, T. I. Sølling, M. M. Nielsen, O. Bunk, K. Kjaer, N. Tchebotareva, M. D. Watson, K. Müllen and J. Piris, *Langmuir*, 2004, **20**, 4039–4146.
39 N. Reitzel, T. Hassenkam, K. Balashev, T. R. Jensen, P. B. Howes, K. Kjaer, A. Fechtenkotter, N. Tchebotareva, S. Ito, K. Müllen and T. Bjørnholm, *Chem. Eur. J.*, 2001, **7**, 4894–4901.
40 K. Nørgaard, *PhD thesis*, Copenhagen, 2004.
41 K. Nørgaard, N. Stuhr-Hansen, T. Bjû¡rnholm, M. J. Weygand and K. Kjaer, *HASYLAB Annual report*, 2002. http://www-hasylab.desy.de/science/annual_reports/2002_report/.
42 M. Brust, M. Walker, D. Bethell, D. J. Schiffrin and R. Whyman, *J. Chem. Soc., Chem. Commun.*, 1994, **7**, 801.
43 A. Bezryadin, C. Dekker and G. Schmid, *Appl. Phys. Lett.*, 1997, **71**, 1273.
44 K. Nørgaard, M. J. Weygand, K. Kjaer, M. Brust and T. Bjørnholm, *Faraday Discuss.*, 2004, **125**, 221–233.
45 A. C. Templeton, M. P. Wuelfing and R. W. Murray, *Acc. Chem. Res.*, 2000, **33**, 27.
46 A. K. Boal and V. M. Rotello, *J. Am. Chem. Soc.*, 2000, **122**, 734.
47 M. H. V. Werts, H. Zaim and M. Blanchard-Desce, *Photochem. Photobiol. Sci.*, 2004, **3**, 29–32.
48 A. Badia, L. Cuccia, L. Demers, F. Morin and R. B. Lennox, *J. Am. Chem. Soc.*, 1997, **119**, 2682.
49 H. Sirringhaus, P. J. Brown, R. H. Friend, M. M. Nielsen, K. Bechgaard, B. M. W. Langeveld-Voss, A. J. H. Spiering, R. A. J. Janssen, E. W. Meijer, P. Herwig and D. M. de Leeuw, *Nature*, 1999, **401**, 685–688.
50 M. Nonnenmacher, M. P. Oboyle and H. K. Wickramasinghe, *Appl. Phys. Lett.*, 1991, **58**, 2921–2923.
51 T. Hassenkam, D. R. Greve and T. Bjørnholm, *Adv. Mater.*, 2001, **13**, 631–634.
52 M. J. Loiacono, E. L. Granstrom and C. D. Frisbie, *J. Phys. Chem. B*, 1998, **102**, 1679.
53 M. Brust and C. J. Kiely, *Colloids Surf., A*, 2002, **202**, 175.
54 N. Stuhr-Hansen, J. B. Christensen, N. Harrit and T. Bjørnholm, *J. Org. Chem.*, 2002, **68**, 1275.
55 N. Stuhr-Hansen, *Synth. Commun.*, 2003, **33**, 641–646.
56 L. A. Bumm, J. J. Arnold, M. T. Cygan, T. D. Dunbar, T. P. Burgin, L. Jones, D. L. Allara, J. M. Tour and P. S. Weiss, *Science*, 1996, **271**, 1705–1707.
57 M. A. Reed, C. Zhou, C. J. Muller, T. P. Burgin and J. M. Tour, *Science*, 1997, **278**, 252–254.
58 A. Nitzan and M. A. Ratner, *Science*, 2003, **300**, 1384–1389.
59 R. H. M. Smit, Y. Noat, C. Untiedt, N. D. Lang, M. C. van Hemert and J. M. van Ruitenbeek, *Nature*, 2002, **419**, 906–909.
60 H. Park, J. Park, A. K. L. Lim, E. H. Anderson, A. P. Alivisatos and P. L. McEuen, *Nature*, 2000, **407**, 57–60.
61 J. Park, A. N. Pasupathy, J. I. Goldsmith, C. Chang, Y. Yaish, J. R. Petta, M. Rinkoski, J. P. Sethna, H. D. Abruna, P. L. McEuen and D. C. Ralph, *Nature*, 2002, **417**, 722–725.
62 S. Kubatkin, A. Danilov, M. Hjort, J. Cornil, J. L. Bredas, N. Stuhr-Hansen, P. Hedegård and T. Bjørnholm, *Nature*, 2003, **425**, 698–701.
63 Ö. Turel, J. H. Lee, X. Ma and K. K. Likharev, *Int. J. Circ. Theor. Appl.*, 2004, **32**, 277–302.
64 J. M. Tour, W. L. Van Zandt, C. P. Husband, S. M. Husband, L. S. Wilson, P. D. Franzon and D. P. Nackashi, *IEEE Trans. Nanotechnol.*, 2002, **1**, 100–109.

This journal is © The Royal Society of Chemistry 2005